Experimental investigation and analysis of human femur Implant in hemiarthroplasty for equivalent stress during walking and stumbling conditions for PEEK, CFR-PEEK and Ti-6Al-4V materials

[1]Dr.Shailesh S.Pimpale, [2]Dr.Manish S.Deshmukh, [3]Prof.Rupesh S. Sundge, [4]Prof. Pankaj L. Firake, [5]Dr.Vithoba T. Tale , [6]Dr. Pruthviraj D. Patil

[1]Associate Professor,Department of Mechanical Engineering,JSPM'S Rajarshi Shahu College of Engineering,Pune- Maharashtra,India; sspimpale_mech@jspmrscoe.edu.in ;
[2]Professor,Department of Mechanical Engineering,AISSMS College of Engineering,Pune-Maharashtra,India; msdeshmukh@aissmscoe.com;
[3]Assistant Professor,Department of Mechanical Engineering,JSPM'S Rajarshi Shahu College of Engineering,Pune- Maharashtra,India; rssundge_mech@jspmrscoe.edu.in;
[4] Assistant Professor,Department of Mechanical Engineering,JSPM'S Rajarshi Shahu College of Engineering,Pune- Maharashtra,India; plfirake_mech@jspmrscoe.edu.in;
[5] Professor,Department of Mechanical Engineering,JSPM'S Rajarshi Shahu College of Engineering,Pune- Maharashtra,India; vttale_mech@jspmrscoe.edu.in;
[6] Assistant Professor,Department of Mechanical Engineering,JSPM'S Rajarshi Shahu College of Engineering,Pune- Maharashtra,India; pdpatil_mech@jspmrscoe.edu.in.

Abstract: The fatigue and wear analysis of femur implant in hip hemiarthroplasty plays substantial role in estimating the life of implant and in selection of idea material. This study comprises modeling and finite element analysis of femur head, which is utilized in hip hemiarthroplasty. The materials utilized in analysis are polyether-ether-ketone (PEEK), carbon-fiber-reinforced polyether-ether-ketone (CFR-PEEK) and titanium alloy (Ti-6Al-4V), the dynamic loading under the human activities as walking barefoot, stumbling. The FEA was performed in ANSYS Workbench 19.2 and modeling was carried out on SolidWorks 2021. The S-N curves were utilized for the fatigue life estimation and modified Archard's law was utilized for accounting the wear depth per year. The result obtained from FEA were equivalent stress, contact pressure and sliding distance for all materials and activities. After observing the results, it is concluded that the CFR PEEK is ideal for the femur head under all activities and the higher stresses and contact pressures were generated under stumbling activity. The approximated life of the CFR PEEK material femur head was 10 years, after that it is required to be changed or replaced for smooth functionality.
Keywords: Hemiarthroplasty, Femur Implant, Fatigue Analysis, Wear Analysis.

1. Introduction

Extensive research is being performed on the application of the cobalt chromium molybdenum (CoCrMo) and ultra-high molecular weight polyethylene (UHMWPE) materials in the hip arthroplasty for enhancing the fatigue life and reducing the wear. Researchers have investigated the biocompatibility of the surface engineered Ti6Al4V material femoral heads utilized as hip implants. It is discovered that the femoral heads have lower life and changing them overtime is traumatizing for the patients (specifically patients with old age). There biocompatibility is investigated with respect to wear, corrosion and fatigue resistance. The effect of the surface treatment on the fatigue life and wear resistance is also investigated. It was concluded that the surface treatment substantially improved the wear, corrosion and fatigue resistance of the femoral heads [1]–[6]. In a study, the assessment of fatigue life of cemented hip prosthesis is carried out through finite element approach based on three-dimensional scanned data. The three-dimensional scanned data was utilized of the modelling of the hip prosthesis. The fatigue life of the hip implant components till crack initiation and loosening were studied through finite element analysis. The concentration of high tensile stresses was discovered in the region of crack initiation. This can also be employed by other researchers for assessing the fatigue life of the femoral head and hip prosthesis components [7]–[12].In a study, hip joint implant consisting CoCr alloy backing and UHMWPE acetabular cup is analyzed for estimating the wear through utilizing modified Archard's law. The finite element analysis was carried out in ANSYS 18.0. the body weights were varied for the analysis, which results in to varying loads. After analyzing different combinations of materials for backing and acetabular cup, it was discovered that the high stresses were found in CoCr alloy backing and UHMWPE acetabular cup [13]–[18]. The hip hemiarthroplastycomprises the femur head as implant material and acetabulum cup is the original cortical bone. In case of total hip arthroplasty the acetabulum cup also comprises different implant material and sometime need liner between the femur head and acetabulum cup [19]–[25].The difference between the hemiarthroplasty and total arthroplastyis shown in **Figure 1.**

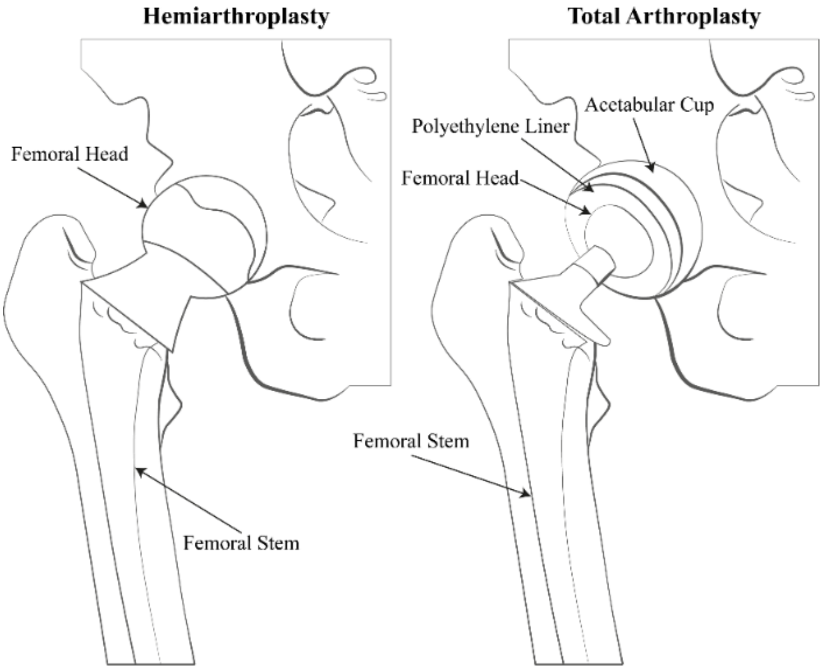

Fig 1: Hemiarthroplasty and total arthroplastywith femur prothesis.

The polyether-ether-ketone (PEEK) is polymer material, which comprises substantia biocompatibility and is lighter in weight. It is extensively applied as dental, hip or other prothesis implants. In a study, a review is carried out on the biocompatibility and utilization of PEEK in removable or fixed prothesis. It was discovered that the PEEK comprises mechanical properties nearer to bone and comprises significant biocompatibility. They were found to be better material for dental implant as comparable to titanium alloys [26]–[32]. Researchers have examined the properties of the cortical bone through ultrasound assessment. The outcomes comprise better understanding of the bone fragility and assessing its properties. It was discovered the recent technologies utilized for assessing the cortical bone properties are lacking accuracy and can just measure the thickness and bulk wave velocities of bone [33]–[39]. In a study, the utilization of the PEEK and CFR PEEK material as replacement to UHMWPE in case of total knee replacement is examined experimentally. The wear in the PEEK and CFR PEEK material is investigated with respect to knee replacement and compared with UHMWPE. The wear rates obtained in the PEEK and CFR PEEK materials were higher than UHMWPE under same operation. The experimentation simulation was carried out through pin-on-plate method or experiment. It was discovered that the PEEK and CFR PEEK materials comprises lower life as comparable to UHMWPE, but can be applied as replacement in high-conformity designs [40]–[45]. In a study, the Ti-6Al-4V extra low interstitials alloy utilized as total hip replacement implant is examined for the fatigue and fracture strength through FEM. The stem neck was concentrated in this study, as the lesser the thickness, the lower structural integrity. The five different model with different neck thickness were utilized for performing the FEM. The stress-strain and fatigue crack growth were assessed through finite element method (FEM) and extended (XFEM). It was discovered that the stress intensity was higher at the neck region and the model with 9 mm more thickness with respect to original one has higher fatigue strength. It was also discovered that the reverse engineered 3D model was more efficient in modelling the implant [46]–[52].

2. Finite Element Analysis (FEA)

The hip joint is simulated in ANSYS Workbench 19.2 commercial package and the FEA is performed. The modeling of the 3D model is carried out in SolidWorks 2021, which is shown in **Figure2.** The material properties along with the S-N curve data is utilized for the dynamic fatigue analysis. The loads for the activities walking, stumbling, is utilized as dynamic loading for replicating the loading during these activities on the femur head. Further, the boundary conditions are applied for constraining the mathematical model. The meshing is applied with respect to element size for optimum aspect ratio. The Von Mises (Equivalent) stress, total deformation, contact pressure and sliding distances are evaluated for each material and each activity through the FEA. The time required for the solution was 35 min with 16Gb ram and 2.3 GHz processer.

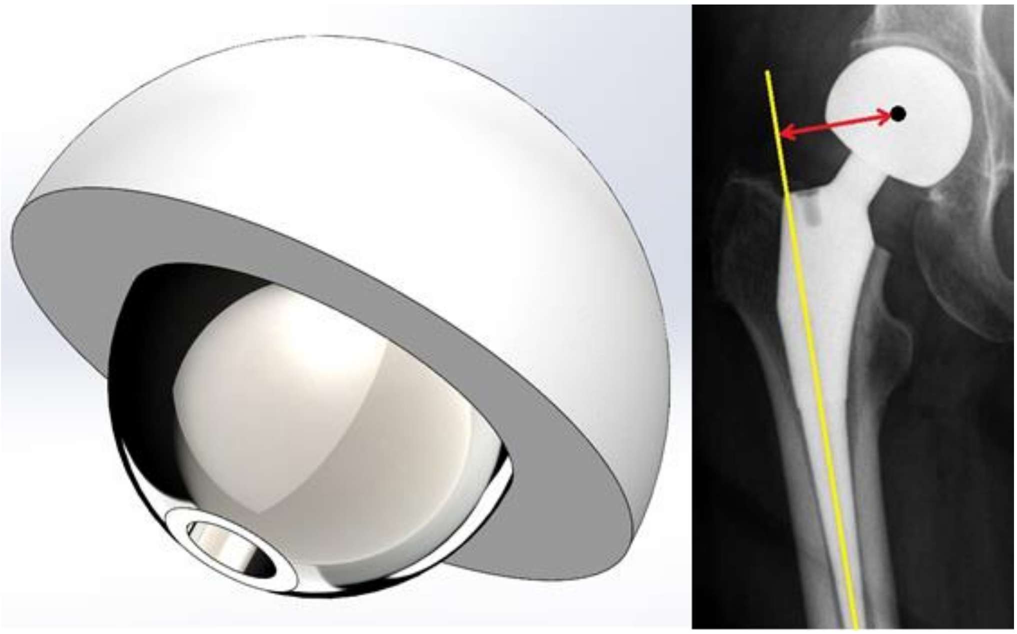

Fig 2: Hip hemiarthroplasty implant 3D model.

3. Material Properties

The materials utilized for the femur head prothesis in this study are polyether ether ketone (PEEK), carbon-fiber-reinforced polyether ether ketone (CFR-PEEK) and Ti-6Al-4V titanium alloy. The acetabulum is the cortical bone of the hip, as the arthroplasty is considered in this study is hip hemiarthroplasty. The properties of all the materials utilized in this study are given in **Table1.** The properties of the cortical bone are adopted from the studies comprises the assessment of properties of the bone in healthy and deceased condition [33], [53]. The PEEK and CFR PEEK materials have similar properties with a significant difference, there properties are adopted form the studies comprising there applications and experimentation evaluation for biocompatibility [26], [40], [54]. The properties of titanium alloy are referred form the studies comprising its fatigue, wear and tribological properties assessment for hip implant [46], [55]–[57].

Table 1: PEEK, CFR PEEK and titanium alloy properties.

Property	Value	Unit
Cortical Bone		
Density	2	g/cm^3
Isotropic Elasticity		
Young's Modulus	14000	MPa
Poisson's Ratio	0.4	
Bulk Modulus	2.3333E+04	MPa
Shear Modulus	5E+03	MPa
Tensile Yield Strength	104	MPa
Tensile Ultimate Strength	150	MPa
PEEK		
Density	1.3	g/cm^3
Isotropic Elasticity		
Young's Modulus	4000	MPa
Poisson's Ratio	0.32	
Bulk Modulus	3.7037E+03	MPa
Shear Modulus	1.5152E+03	MPa
Tensile Yield Strength	80	MPa
Tensile Ultimate Strength	120	MPa
CFR PEEK		
Density	1.4	Kg/m^3
Isotropic Elasticity		
Young's Modulus	18000	MPa
Poisson's Ratio	0.32	
Bulk Modulus	1.6667E+04	MPa
Shear Modulus	6.8182E+03	MPa
Tensile Yield Strength	120	MPa
Tensile Ultimate Strength	160	MPa
Ti-6Al-4V		
Density	4.512	g/cm^3
Isotropic Elasticity		
Young's Modulus	1.1E+05	MPa
Poisson's Ratio	0.32	
Bulk Modulus	1.0185E+05	MPa
Shear Modulus	4.1667E+04	MPa
Tensile Yield Strength	800	MPa
Tensile Ultimate Strength	800	MPa

The Wohler S-N diagram comprises the graph of stress versus number of cycles to failure, this diagram is tested through several methods and is dissimilar with respect to materials. This graph is a log-log plot of the stresses with respect to number of cycles. The S-N curve comprises an event where the curve gets flatten, that stress is known as endurance limit. Endurance limit means under this stress the life of the component is infinite. The S-N data for the cortical bone is adopted from the study comprising the fatigue analysis of human cortical bone through rotating cantilever fatigue tests [58].The S-N graph of the cortical bone material is shown in **Figure3.** The S-N data for the PEEK and CFR PEEK is adopted from the study comprising the fatigue analysis of notched samples of PEEK and CFR PEEK under tension loading through fractographic analysis [59]. The S-N graph of the PEEK and CFR PEEK material is shown in **Figure4.**The S-N data for the titanium alloy (Ti-6Al-4V) is adopted from the study comprising the fatigue analysis of hip transplant stem with Ti-6Al-4V and cobalt-chromium alloy materials [60]. The S-N graph of the titanium alloy (Ti-6Al-4V) material is shown in **Figure5.**

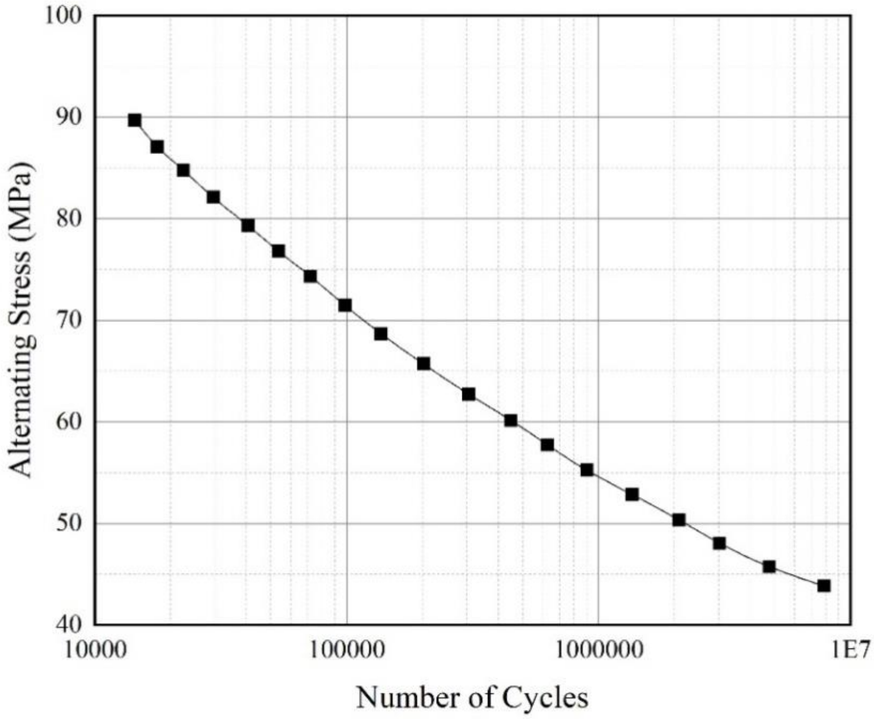

Fig 3: Alternating Stress Vs number of cycles graph of cortical bone.[59]

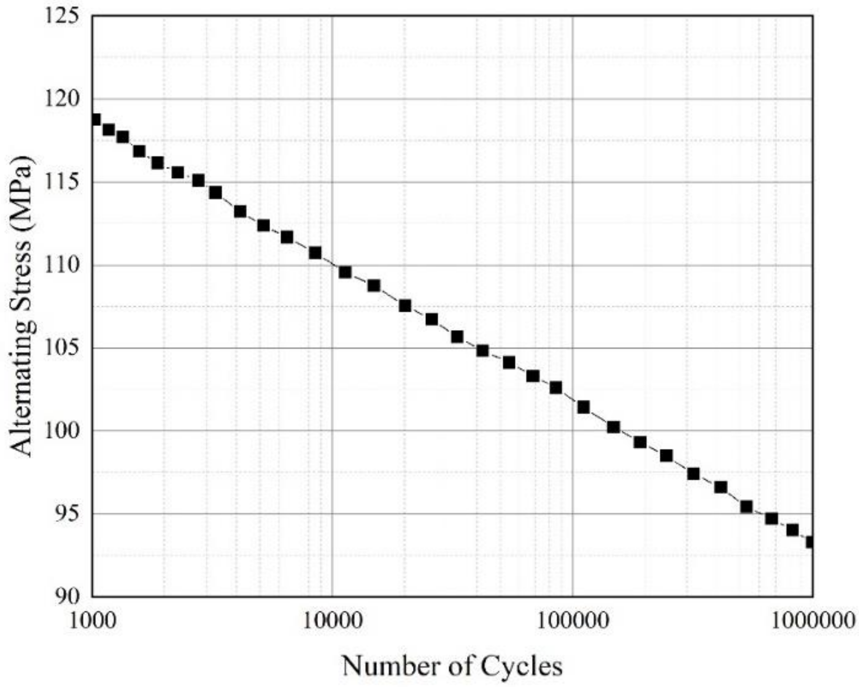

Fig 4: Alternating Stress Vs number of cycles graph of PEEK and CFR PEEK.[59]

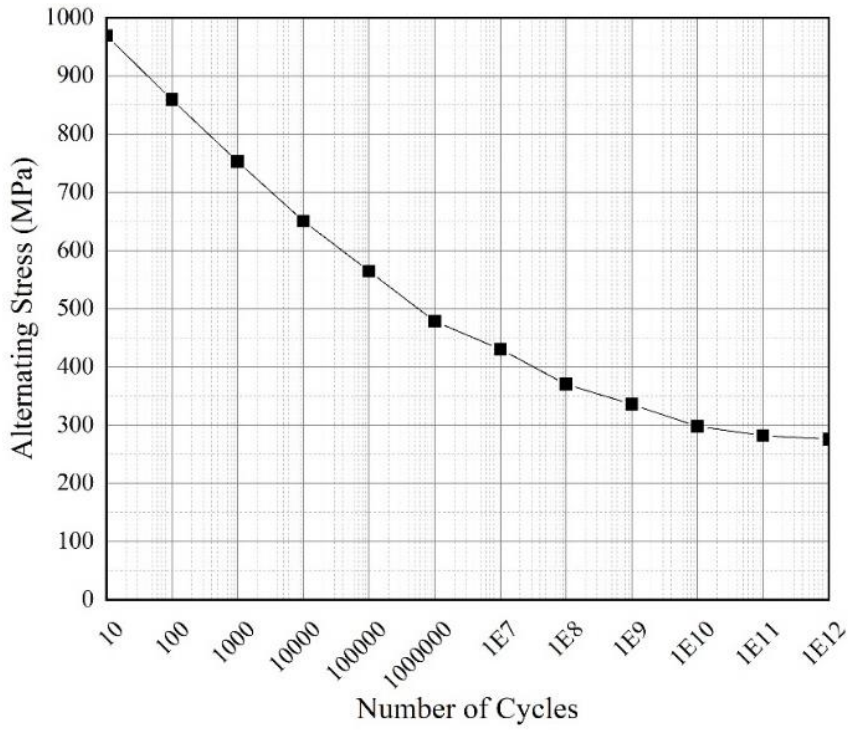

Fig 5: Alternating Stress Vs number of cycles graph of titanium alloy.[60]

4. Loads and Boundary Conditions

The activities considered for dynamic analysis in this study are walking bare foot, stumbling. The loads acting on the femur head during these activities are adopted form the study comprising the load analysis of weight and different activities on the hip joint and femur head [61]–[65]. The dynamic force applied on the femur head X, Y and Z direction with respect to time during walking activity is shown in **Figure6.** The dynamic force applied on the femur head X, Y and Z direction with respect to time during stumbling activity is shown in **Figure7.**

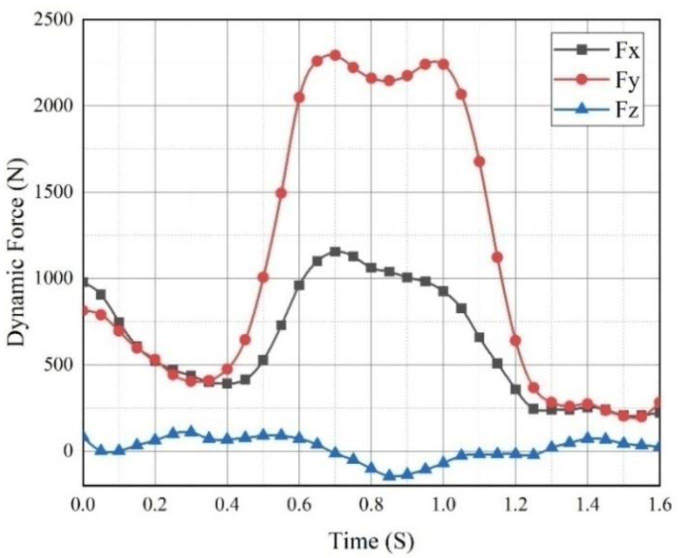

Fig 6: Dynamic force in X, Y and Z directions with respect to time for walking barefoot activity.[63]

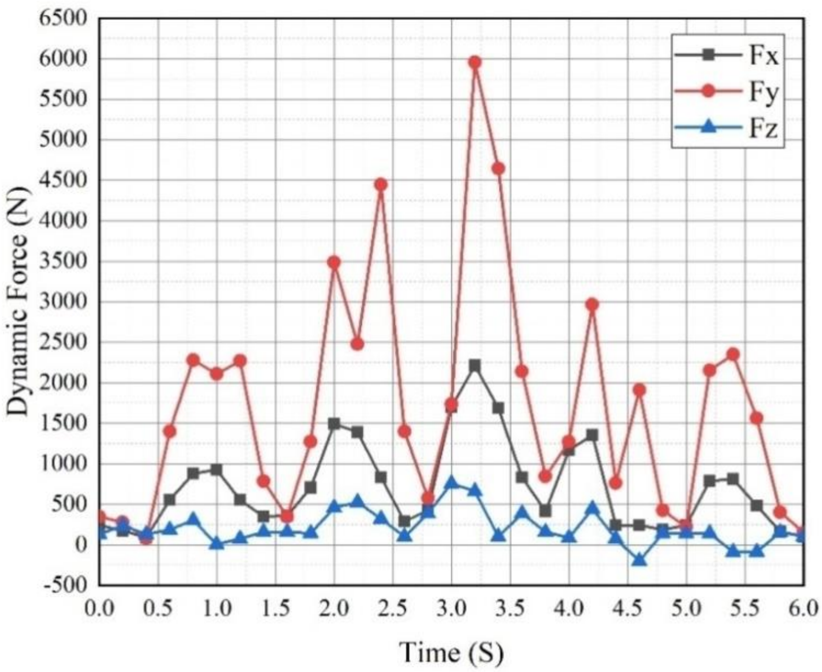

Fig 7: Dynamic force in X, Y and Z directions with respect to time for stumbling activity.[63]

The boundary conditions applied for the FEA are fixed acetabulum and force is applied on the femur head, where the stem is connected to it. The material assignment for the acetabulum is kept constant as cortical bone material and the femur head material assignments is change with PEEK, CFR PEEK and titanium alloy. The boundary conditions are shown in **Figure8.** The contact surface between the acetabulum and the femur head is hemispherical and assigned with friction coefficient as 0.1, as the friction between them is minimal due lubricant in vivo operation. The contact surface assignment as frictional contact is shown in **Figure 9.**

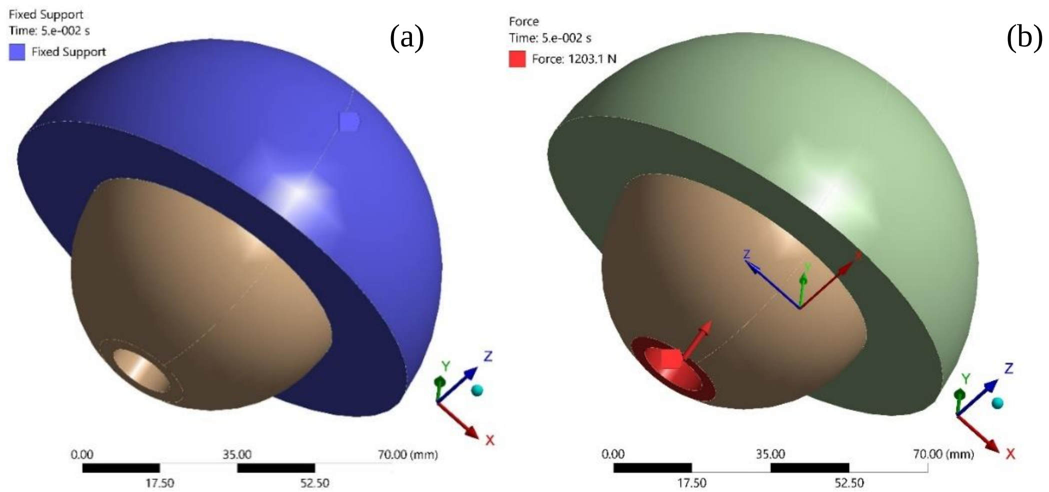

Fig 8: Boundary conditions (a) Fixed support, and (b) Dynamic force application.

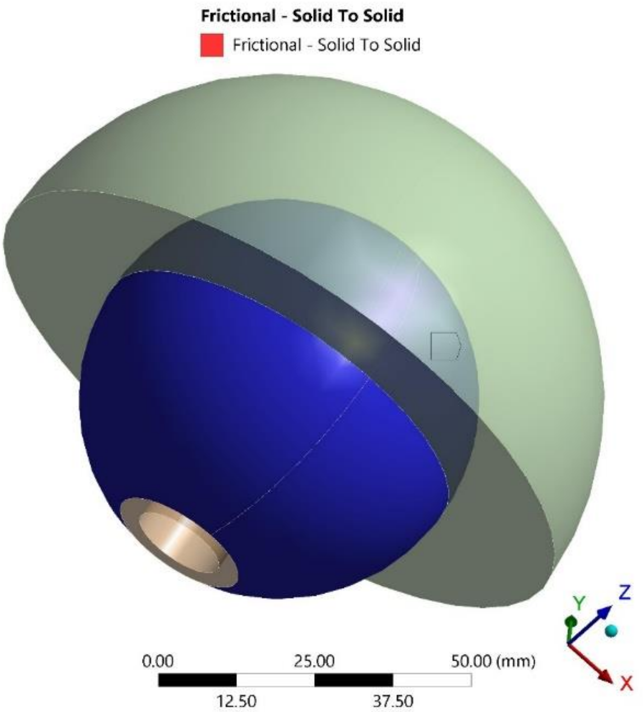

Fig 9: Frictional contact between femur head and acetabulum.

5. FEA Results

5.1. Equivalent Stress

The results obtained from the FEA comprise the equivalent stress, the maximum equivalent stress obtained for walking activity at 1.6 s time for material PEEK. CFR PEEK and Ti-6Al-4V are 11.502, 13.188 and 11.329 MPa respectively, which is shown in **Figure10.** The maximum equivalent stress obtained during the walking activity for PEEK, CFR PEEK and Ti-6Al-4V are 13.216, 14.839 and 12.922 MPa respectively, which is shown in **Figure 11.** The maximum equivalent stress occurred during the walking activity for PEEK, CFR PEEK and Ti-6Al-4V were at time 1.05, 1 and 1 s respectively. Similarly, the minimum equivalent stress obtained during the walking activity for PEEK, CFR PEEK and Ti-6Al-4V are 1.6747, 3.7543 and 4.6244MParespectively, and were occurred at time 0.35, 0.3 and 0.5 s respectively.

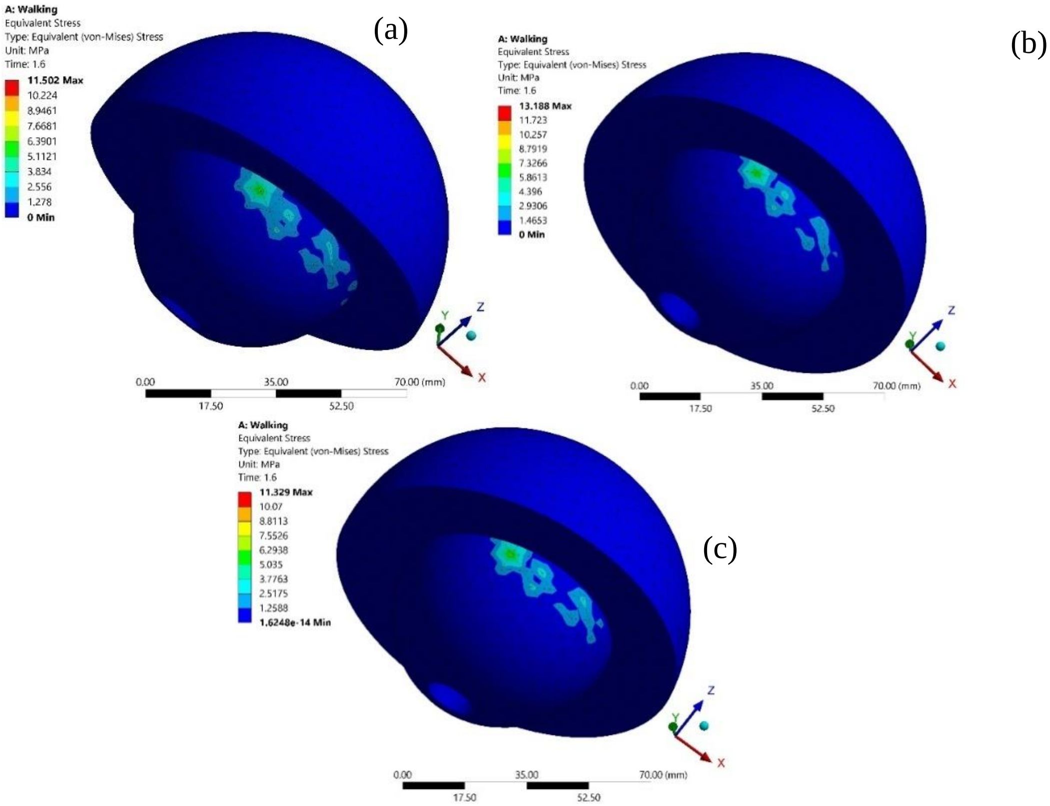

Fig 10: Equivalent stress during walking activity for (a) PEEK, (b) CFR PEEK and (c) Ti-6Al-4V.

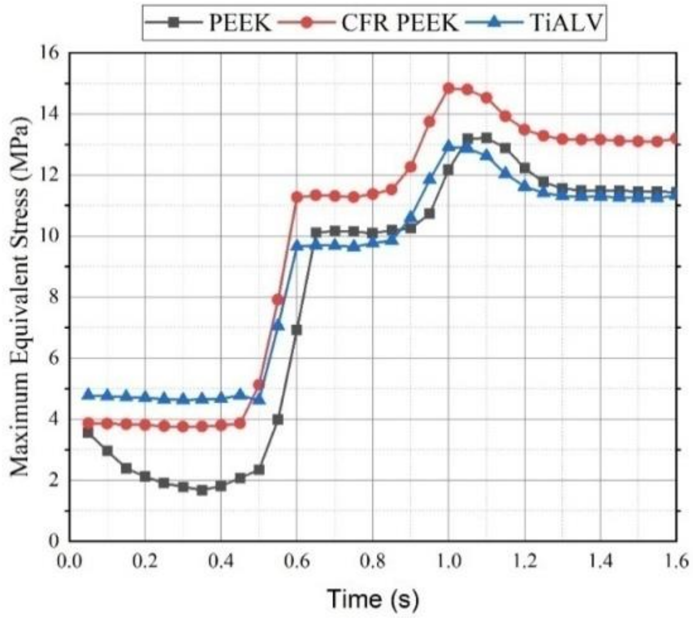

Fig 11: Equivalent stress with respect to time during walking activity for PEEK, CFR PEEK and Ti-6Al-4V.

The maximum equivalent stress obtained for stumbling activity at 6s time for material PEEK. CFR PEEK and Ti-6Al-4V are 250.83, 92 and 243.09 MPa respectively, which is shown in **Figure 12.** The maximum equivalent stress obtained during the stumbling activity for PEEK, CFR PEEK and Ti-6Al-4V are 257.5, 104.95 and 85.693 MPa respectively, which is shown in **Figure 13.** The maximum equivalent stress occurred during the stumbling activity for PEEK, CFR PEEK and Ti-6Al-4V were at time 3.2 s. Similarly, the minimum equivalent stress obtained during the stumbling activity for PEEK, CFR PEEK and Ti-6Al-4V are 3.2954, 2.4563 and 1.7914 MPa respectively, and were occurred at time 0.4 s.

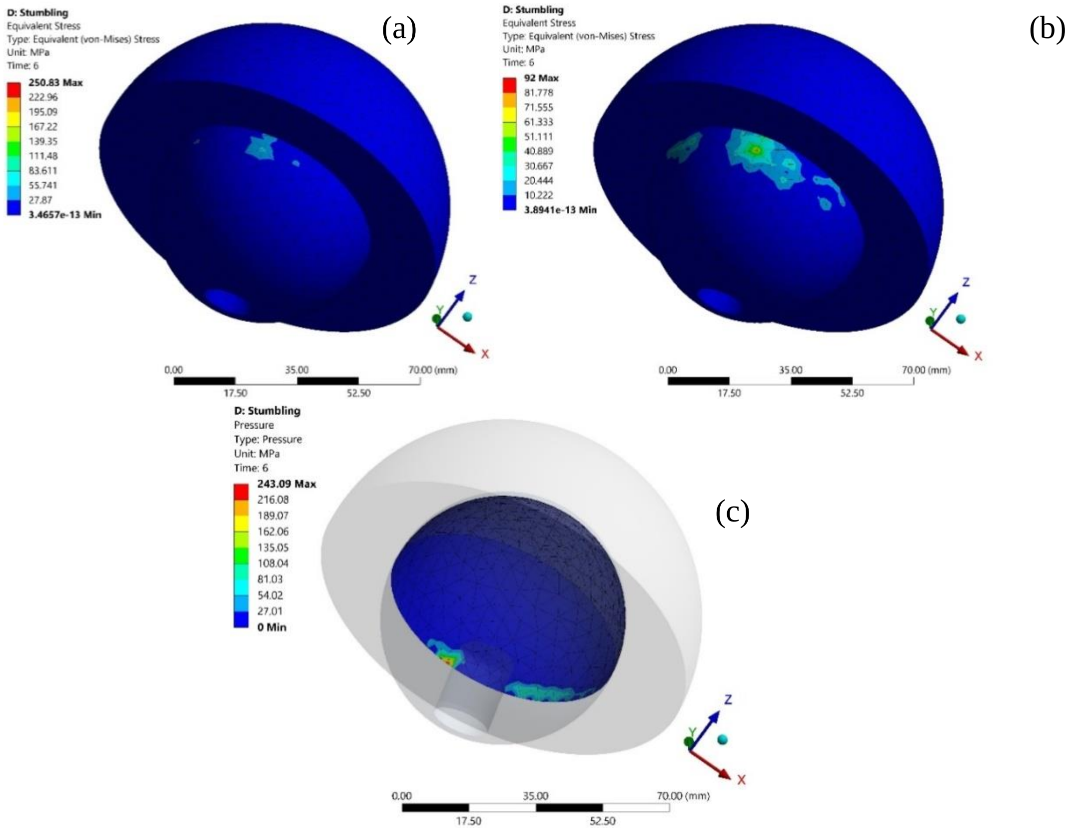

Fig 82: Equivalent stress during stumbling activity for (a) PEEK, (b) CFR PEEK and (c) Ti-6Al-4V.

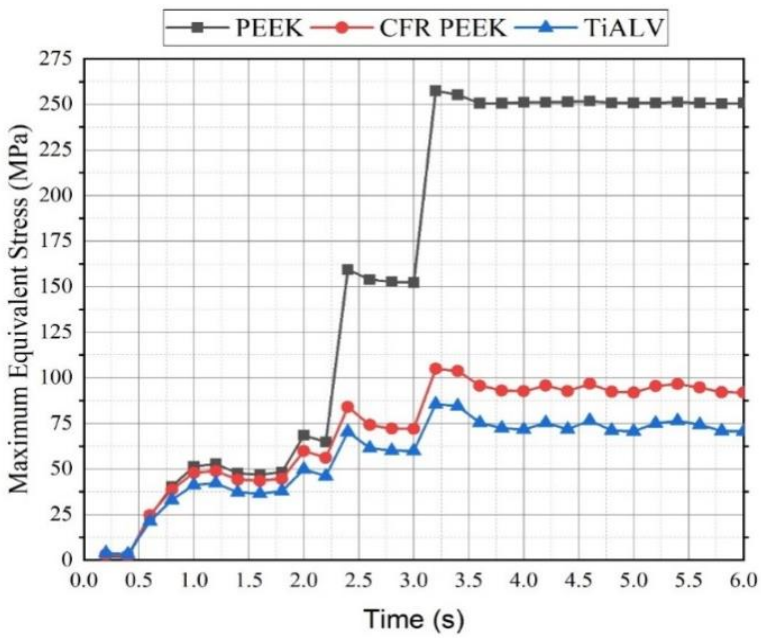

Fig 93: Equivalent stress with respect to time during stumbling activity for PEEK, CFR PEEK and Ti-6Al-4V.

6. Fatigue Analysis

The fatigue analysis comprises utilization of the S-N curves for the calculation of the life of the femur head in cycles with respect to different material assignment. The estimation of the fatigue life consists the calculation of mean stress (σ_m) and alternating stress (σ_a), which are calculated through following formula:

$$\sigma_m = 0.5(\sigma_{max} + \sigma_{min})$$
$$\sigma_a = 0.5(\sigma_{max} - \sigma_{min})$$

Where, σ_m is mean stress,
$\sigma_a$is alternating stress,
$\sigma_{max}$is maximum stress
andσ_{min} is minimum stress.

Table 2: The mean and alternating stress with respect to activities and materials.

Activity	Material	Mean Stress (MPa)	Alternating Stress (Mpa)
Walking	PEEK	7.44535	5.77065
	CFR PEEK	9.29665	5.54235
	Ti-6Al-4V	8.7732	4.1488
Stumbling	PEEK	129.646	127.854
	CFR PEEK	53.7032	51.2469
	Ti-6Al-4V	44.4942	41.1988

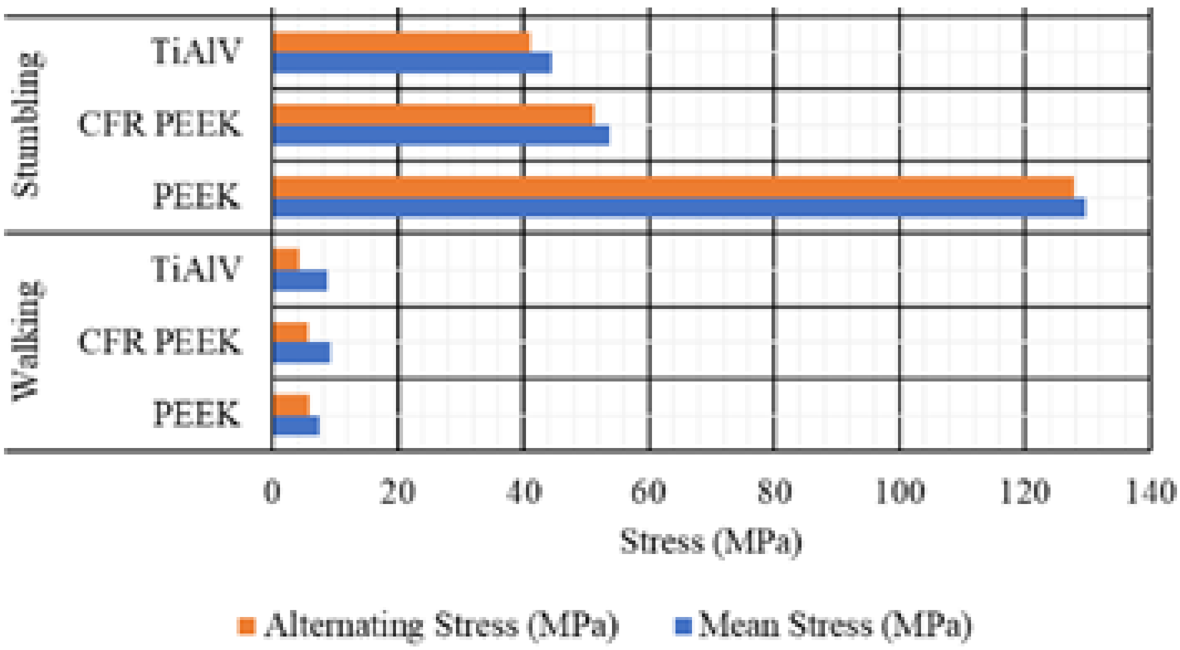

Fig 14: Alternating and mean stress with respect to activities and materials.

7. Wear Analysis

The undesirable material loss from the surface of any body is known as wear. The wear in case of prosthesis is affected through several parameters, such as contact status, contact pressure, sliding distance and surface or tribological properties of the body. The wear behavior in case of plastic sliding on metal, this type of wear comprises three stages namely wear-in period, steady state period and severe wear period. The wear-in period consists shearing of plastic material and production of wear debris. In steady state period, this wear debris forms layer between the interface of contact and wear is in form of adhesion in the surfaces. The severe wear is also known as fatigue wear, which causes when the contact stress is higher than the yield strength of the material [66]–[76]. For the purpose of estimation, the wear rate many models were developed, but the Archard's law is utilized in this study for the estimation wear behavior and mechanism [77]–[79]. The following equation is utilized for estimating the wear [80]:

$$V = K_w S P_n$$

Where, the V is total volume of wear generated,
$K_w$is wear coefficient,
Sis sliding distance
andP_n is normal pressure.
The above equation clearly defines that the wear is corelated to the material properties and the motion. The wear depth and contact surface vary with the motion in case of femoral head and acetabular, the Archard's equation is required to be modified in incremental form:

$$dV = \Delta A dh = K_w \times \sigma \times \Delta A \times ds$$
$$dh = K_w \times \sigma \times ds$$

Where, dV is increment of wear volume,
ΔAis infinitesimal contact area,
$K_w$is wear coefficient,
dhis infinitesimal wear depth,
dsis infinitesimal sliding distance
andσ is normal contact stresses.

The K_w is wear coefficient, which is function of material properties and counter face roughness and can be calculated through experimentation. The value of the wear coefficient is adopted form pin on disk experiment [81]-[82] and it is 3.5E-07 mm^3/Nm.Further the sliding distance is estimated through utilizing the walking cycle analysis. The walking cycle comprises the motion like the hip flexion, extension, adduction, abduction and rotation internally or externally. The highest contribution of the motion in the walking cycle is of flexion and extension motion as comparable to other motions. The reduction in the angle of the anterior surfaces of bones is caused by the flexion and it also known as folding crusade. The straightening involved in the flexion is known as extension. The angle of flexion and extension the half walking cycle are 23° and 17° respectively and in case of full walking cycle the joint has rotation of total 80°. In this study, the radius of femur head is considered to be 32 mm.

$$\text{Total hip rotation in single cycle} = 80° = 1.396 \text{ radians}$$
$$\text{Sliding Distance (ds)} = \text{Head Radius} \times \text{Rotation Angle}$$
$$= 32 \times 1.396 = 44.672 \text{ mm}$$
$$= 44.672 \text{ E-03 m}$$

Through utilizing the Archard's law, the wear depth is calculated as:

$$\text{Wear Depth (dh)} = K_w \times \sigma \times ds$$
$$= 3.5E - 07 \times \sigma \times 44.672E - 03$$

Table 3: Wear depth and life in years with respect to activities and materials.

Activity	Material	Maximum Contact Pressure (MPa)	Wear Depth (mm/year)	Life in year
Walking	PEEK	12.5136	0.195653	10.2
	CFR PEEK	14.355	0.224443	9
	Ti-6Al-4V	12.4803	0.195132	10.2
Stumbling	PEEK	261.306	4.085572	0.5
	CFR PEEK	99.513	1.555906	1.2
	Ti-6Al-4V	79.743	1.246798	1.6

The wear depths for each activity with respect to material is calculated through wear depth equation, these obtained values are presented in **Table. 3.**If the average walking cycle considered as 1000000 (one million) steps (cycles) are taken by a human. The obtained wear depths are converted in mm per year and presented in **Table. 3.**The maximum allowable wear in this study is considered as 2 mm, as more than this can affect the functionality of the transplant causing noises while walking. Finally, through wear depth and allowable wear the life of the respective materials assigned and activities, the life in years is calculated and presented in **Table. 3.**

8. Discussions

The results obtained from the FEA are tabulated in **Table. 4**, where the maximum equivalent stress, sliding distance, contact pressure and minimum equivalent stress with respect to activities and materials is observed. It is discovered that in walking activity the maximum equivalent stress, minimum equivalent stress and maximum contact pressure for CFR PEEK is higher than other materials, but the maximum sliding distance for PEEK is higher than others. In case of stumbling activity, it is observed that the maximum equivalent stress for PEEK, minimum equivalent stress for Ti-6Al-4V, maximum contact pressure for PEEK and maximum sliding distance for PEEK is higher as compared with other materials. The highest stress and contact pressure is obtained in stumbling activity for PEEK material as comparable to other materials, which can be seen in **Figure15.**

Table 4: The maximum equivalent stress, sliding distance, contact pressure and minimum equivalent stress with respect to activities and materials.

Activity	Material	Maximum Equivalent Stress (MPa)	Minimum Equivalent Stress (MPa)	Maximum Contact Pressure (MPa)	Maximum Sliding Distance (mm)
Walking	PEEK	13.216	1.6747	12.5136	78.271
	CFR PEEK	14.839	3.7543	14.355	20.024
	Ti-6Al-4V	12.922	4.6244	12.4803	13.712
Stumbling	PEEK	257.5	1.7914	261.306	505.25
	CFR PEEK	104.95	2.4563	99.513	161.45
	Ti-6Al-4V	85.693	3.2954	79.743	122.64

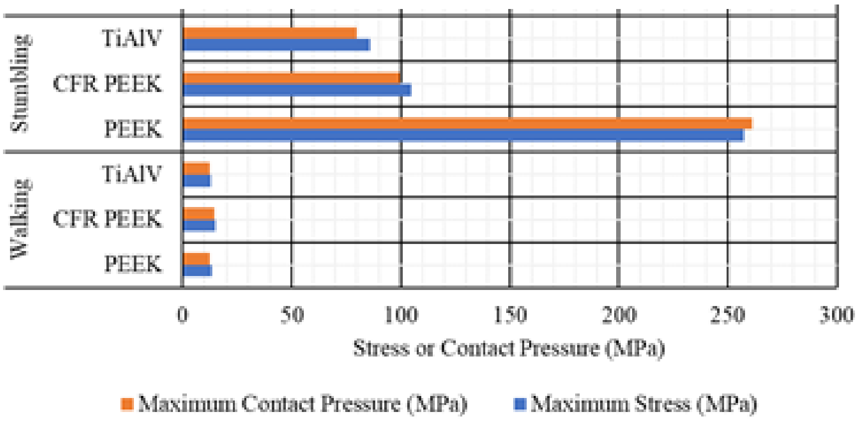

Fig 15: The maximum equivalent stress and contact pressure with respect to activities and materials.

9. Conclusion

In this study the wear and fatigue analysis are performed on the femur head with respect to three materials and four activities. Initially the femur head with 32 mm diameter is modeled and analyzed dynamically with respect to S-N curve, material data and dynamic loads. The numerical analysis is carried for the wear and fatigue life estimation. Some of the key observations are listed below:

- It is discovered that the CFR PEEK material comprises lower life with wear analysis and higher with respect fatigue analysis.
- The highest total deformation is obtained for PEEK material under stumbling activity loading.
- The highest equivalent stress and contact pressure is obtained for PEEK material under stumbling activity loading.
- The equivalent stress and contact pressure were moderate for CFR PEEK material under all activities.
- The equivalent stress and contact pressure were lower for Ti-6Al-4V material under all activities.
- The life obtained with respect to allowable wear depth is higher for Ti-6Al-4V material under all activities.
- The life obtained with respect to allowable wear depth is lower for CFR PEEK material under all activities.
- The life obtained with respect to allowable wear depth is moderate for PEEK material under all activities.

After observing all the outcomes some conclusions are obtained, which are listed below:

- The material ideal for femur head is CFR PEEK, after considering the fatigue and wear depth life, and also the weight to strength ratio.
- The stress and contact pressure are higher under the stumbling activity loading.
- The average life for the femur head with CFR PEEK material, after observing all the outcomes under all activities is approximately 10 years.

The method performed in this study can further utilized for estimating the significant and most ideal material for the femur head implant or other prothesis.

References

[1] A. Samanta et al., “Biocompatibility and cyclic fatigue response of surface engineered Ti6Al4V femoral heads for hip-implant application,” Ceramics International, vol. 47, no. 5, pp. 6905–6917, Mar. 2021, doi: 10.1016/j.ceramint.2020.11.037.

[2] J. Meng et al., “Friction and wear properties of TiN-TiB2-Ni based composite coatings by argon arc cladding technology,” Surface and Coatings Technology, vol. 374, pp. 437–447, Sep. 2019, doi: 10.1016/j.surfcoat.2019.06.015.

[3] S. Datta, M. Das, V. K. Balla, S. Bodhak, and V. K. Murugesan, “Mechanical, wear, corrosion and biological properties of arc deposited titanium nitride coatings,” Surface and Coatings Technology, vol. 344, pp. 214–222, Jun. 2018, doi: 10.1016/j.surfcoat.2018.03.019.

[4] M. Łępicka, M. Grądzka-Dahlke, D. Pieniak, K. Pasierbiewicz, K. Kryńska, and A. Niewczas, “Tribological performance of titanium nitride coatings: A comparative study on TiN-coated stainless steel and titanium alloy,” Wear, vol. 422–423, pp. 68–80, Mar. 2019, doi: 10.1016/j.wear.2019.01.029.

[5] J. Qi, Y. Yang, M. Zhou, Z. Chen, and K. Chen, “Effect of transition layer on the performance of hydroxyapatite/titanium nitride coating developed on Ti-6Al-4V alloy by magnetron sputtering,” Ceramics International, vol. 45, no. 4, pp. 4863–4869, Mar. 2019, doi: 10.1016/j.ceramint.2018.11.183.

[6] S. Mehnath, M. Arjama, M. Rajan, K. Premkumar, K. Karthikeyan, and M. Jeyaraj, “Mineralization of bioactive marine sponge and electrophoretic deposition on Ti-6Al-4V implant for osteointegration,” Surface and Coatings Technology, vol. 392, p. 125727, Jun. 2020, doi: 10.1016/j.surfcoat.2020.125727.

[7] M. Babić, O. Verić, Ž. Božić, and A. Sušić, “Finite element modelling and fatigue life assessment of a cemented total hip prosthesis based on 3D scanning,” Engineering Failure Analysis, vol. 113, p. 104536, Jul. 2020, doi: 10.1016/j.engfailanal.2020.104536.

[8] S. Griza, S. V. dos Santos, M. M. Ueki, F. Bertoni, and T. R. Strohaecker, “Case study and analysis of a fatigue failure in a THA stem,” Engineering Failure Analysis, vol. 28, pp. 166–175, Mar. 2013, doi: 10.1016/j.engfailanal.2012.10.011.

[9] T. Bousnane, S. Benbarek, A. Sahli, B. Serier, and B. A. B. Bouiadjra, “Damage of the Bone-Cement Interface in Finite Element Analyses of Cemented Orthopaedic Implants,” Periodica Polytechnica Mechanical Engineering, vol. 62, no. 2, Art. no. 2, Mar. 2018, doi: 10.3311/PPme.11851.

[10] A. A. Oshkour, M. M. Davoodi, N. A. Abu Osman, Y. H. Yau, F. Tarlochan, and W. A. B. W. Abas, “Finite element analysis of circumferential crack behavior in cement–femoral prosthesis interface,” Materials & Design, vol. 49, pp. 96–102, Aug. 2013, doi: 10.1016/j.matdes.2013.01.037.

[11] O. Kayabasi and F. Erzincanli, “Finite element modelling and analysis of a new cemented hip prosthesis,” Advances in Engineering Software, vol. 37, no. 7, pp. 477–483, Jul. 2006, doi: 10.1016/j.advengsoft.2005.09.003.

[12] T. Achour, M. S. H. Tabeti, M. M. Bouziane, S. Benbarek, B. Bachir Bouiadjra, and A. Mankour, “Finite element analysis of interfacial crack behaviour in cemented total hip arthroplasty,” Computational Materials Science, vol. 47, no. 3, pp. 672–677, Jan. 2010, doi: 10.1016/j.commatsci.2009.10.007.

[13] V. Jangid, A. Kumar Singh, and A. Mishra, “Wear Simulation of Artificial Hip Joints: Effect of Materials,” Materials Today: Proceedings, vol. 18, pp. 3867–3875, Jan. 2019, doi: 10.1016/j.matpr.2019.07.326.

[14] E. Saputra, I. B. Anwar, J. Jamari, and E. van der Heide, “Finite Element Analysis of Artificial Hip Joint Movement During Human Activities,” Procedia Engineering, vol. 68, pp. 102–108, Jan. 2013, doi: 10.1016/j.proeng.2013.12.154.

[15] M. S. Uddin and L. C. Zhang, “Predicting the wear of hard-on-hard hip joint prostheses,” Wear, vol. 301, no. 1, pp. 192–200, Apr. 2013, doi: 10.1016/j.wear.2013.01.009.

[16] M. S. Uddin, C. Y. E. Mak, and S. A. Callary, “Evaluating hip implant wear measurements by CMM technique,” Wear, vol. 364–365, pp. 193–200, Oct. 2016, doi: 10.1016/j.wear.2016.07.017.

[17] W. S. W. Harun et al., “A comprehensive review of hydroxyapatite-based coatings adhesion on metallic biomaterials,” Ceramics International, vol. 44, no. 2, pp. 1250–1268, Feb. 2018, doi: 10.1016/j.ceramint.2017.10.162.

[18] S. Zameer and M. Haneef, “Fatigue Life Estimation of Artificial Hip Joint Model Using Finite Element Method,” Materials Today: Proceedings, vol. 2, no. 4, pp. 2137–2145, Jan. 2015, doi: 10.1016/j.matpr.2015.07.220.

[19] W. Peng, N. Bi, J. Zheng, and N. Xi, "Does total hip arthroplasty provide better outcomes than hemiarthroplasty for the femoral neck fracture? A systematic review and meta-analysis," Chinese Journal of Traumatology, vol. 23, no. 6, pp. 356–362, Dec. 2020, doi: 10.1016/j.cjtee.2020.09.005.

[20] D. You, A. Sepehri, and R. Buckley, "Unipolar or bipolar hip hemiarthroplasty – Which is most efficacious and cost effective?," Injury, vol. 52, no. 4, pp. 671–672, Apr. 2021, doi: 10.1016/j.injury.2020.10.064.

[21] S. Fahad, M. Z. Nawaz Khan, T. Aqueel, and P. Hashmi, "Comparison of bipolar hemiarthroplasty and total hip arthroplasty with dual mobility cup in the treatment of old active patients with displaced neck of femur fracture: A retrospective cohort study," Annals of Medicine and Surgery, vol. 45, pp. 62–65, Sep. 2019, doi: 10.1016/j.amsu.2019.07.025.

[22] J. C. Suarez, W. Arguelles, A. Saxena, P. Rivera, D. Parris, and E. Veledar, "Hemiarthroplasty vs Total Hip Arthroplasty for Femoral Neck Fractures: 2010-2017 Trends in Complication Rates," The Journal of Arthroplasty, vol. 35, no. 6, Supplement, pp. S262–S267, Jun. 2020, doi: 10.1016/j.arth.2020.02.040.

[23] N. M. Hernandez, K. M. Fruth, D. R. Larson, H. M. Kremers, and R. J. Sierra, "Conversion of Failed Hemiarthroplasty to Total Hip Arthroplasty Remains High Risk for Subsequent Complications," The Journal of Arthroplasty, vol. 34, no. 9, pp. 2030–2036, Sep. 2019, doi: 10.1016/j.arth.2019.04.042.

[24] W. Hoskins, S. Rainbird, Y. Peng, S. E. Graves, and R. Bingham, "Hip Hemiarthroplasty for Fractured Neck of Femur Revised to Total Hip Arthroplasty: Outcomes Are Influenced by Patient Age Not Articulation Options," The Journal of Arthroplasty, Apr. 2021, doi: 10.1016/j.arth.2021.04.001.

[25] A. Hernández-Aceituno, M. Ruiz-Álvarez, R. Llorente-Calderón, P. Portilla-Fernández, and A. Figuerola-Tejerina, "Risk factors in total hip arthroplasty and hemiarthroplasty: Infection and mortality," Revista Española de Cirugía Ortopédica y Traumatología (English Edition), vol. 65, no. 4, pp. 239–247, Jul. 2021, doi: 10.1016/j.recote.2021.04.002.

[26] S. Najeeb, M. S. Zafar, Z. Khurshid, and F. Siddiqui, "Applications of polyetheretherketone (PEEK) in oral implantology and prosthodontics," J Prosthodont Res, vol. 60, no. 1, pp. 12–19, Jan. 2016, doi: 10.1016/j.jpor.2015.10.001.

[27] W.-T. Lee, J.-Y.Koak, Y.-J.Lim, S.-K.Kim, H.-B.Kwon, and M.-J. Kim, "Stress shielding and fatigue limits of poly-ether-ether-ketone dental implants," Journal of Biomedical Materials Research Part B: Applied Biomaterials, vol. 100B, no. 4, pp. 1044–1052, 2012, doi: 10.1002/jbm.b.32669.

[28] S. Barkarmo et al., "Nano-hydroxyapatite-coated PEEK implants: A pilot study in rabbit bone," Journal of Biomedical Materials Research Part A, vol. 101A, no. 2, pp. 465–471, 2013, doi: https://doi.org/10.1002/jbm.a.34358.

[29] F. Suska et al., "Enhancement of CRF-PEEK osseointegration by plasma-sprayed hydroxyapatite: A rabbit model," J Biomater Appl, vol. 29, no. 2, pp. 234–242, Aug. 2014, doi: 10.1177/0885328214521669.

[30] A. H. C. Poulsson et al., "Osseointegration of machined, injection moulded and oxygen plasma modified PEEK implants in a sheep model," Biomaterials, vol. 35, no. 12, pp. 3717–3728, Apr. 2014, doi: 10.1016/j.biomaterials.2013.12.056.

[31] S. Costa-Palau, J. Torrents-Nicolas, M. Brufau-de Barberà, and J. Cabratosa-Termes, "Use of polyetheretherketone in the fabrication of a maxillary obturator prosthesis: A clinical report," The Journal of Prosthetic Dentistry, vol. 112, no. 3, pp. 680–682, Sep. 2014, doi: 10.1016/j.prosdent.2013.10.026.

[32] P. A. Staniland, C. J. Wilde, F. A. Bottino, G. Di Pasquale, A. Pollicino, and A. Recca, "Synthesis, characterization and study of the thermal properties of new polyarylene ethers," Polymer, vol. 33, no. 9, pp. 1976–1981, Jan. 1992, doi: 10.1016/0032-3861(92)90503-O.

[33] Q. Grimal and P. Laugier, "Quantitative Ultrasound Assessment of Cortical Bone Properties Beyond Bone Mineral Density," IRBM, vol. 40, no. 1, pp. 16–24, Feb. 2019, doi: 10.1016/j.irbm.2018.10.006.

[34] L. Imbert, J.-C. Aurégan, K. Pernelle, and T. Hoc, "Mechanical and mineral properties of osteogenesis imperfecta human bones at the tissue level," Bone, vol. 65, pp. 18–24, Aug. 2014, doi: 10.1016/j.bone.2014.04.030.

[35] L. A. Ahmed et al., “Measurement of cortical porosity of the proximal femur improves identification of women with nonvertebral fragility fractures,” Osteoporos Int, vol. 26, no. 8, pp. 2137–2146, Aug. 2015, doi: 10.1007/s00198-015-3118-x.

[36] R. Zebaze et al., “Denosumab Reduces Cortical Porosity of the Proximal Femoral Shaft in Postmenopausal Women With Osteoporosis,” Journal of Bone and Mineral Research, vol. 31, no. 10, pp. 1827–1834, 2016, doi: 10.1002/jbmr.2855.

[37] P. Geusens et al., “High-resolution in vivo imaging of bone and joints: a window to microarchitecture,” Nat Rev Rheumatol, vol. 10, no. 5, pp. 304–313, May 2014, doi: 10.1038/nrrheum.2014.23.

[38] D. M. L. Cooper, C. E. Kawalilak, K. Harrison, B. D. Johnston, and J. D. Johnston, “Cortical Bone Porosity: What Is It, Why Is It Important, and How Can We Detect It?,” Curr Osteoporos Rep, vol. 14, no. 5, pp. 187–198, Oct. 2016, doi: 10.1007/s11914-016-0319-y.

[39] S. Bernard, J. Schneider, P. Varga, P. Laugier, K. Raum, and Q. Grimal, “Elasticity–density and viscoelasticity–density relationships at the tibia mid-diaphysis assessed from resonant ultrasound spectroscopy measurements,” Biomech Model Mechanobiol, vol. 15, no. 1, pp. 97–109, Feb. 2016, doi: 10.1007/s10237-015-0689-6.

[40] C. L. Brockett, S. Carbone, J. Fisher, and L. M. Jennings, “PEEK and CFR-PEEK as alternative bearing materials to UHMWPE in a fixed bearing total knee replacement: An experimental wear study,” Wear, vol. 374–375, pp. 86–91, Mar. 2017, doi: 10.1016/j.wear.2016.12.010.

[41] S. A. Atwood, D. W. Van Citters, E. W. Patten, J. Furmanski, M. D. Ries, and L. A. Pruitt, “Tradeoffs amongst fatigue, wear, and oxidation resistance of cross-linked ultra-high molecular weight polyethylene,” Journal of the Mechanical Behavior of Biomedical Materials, vol. 4, no. 7, pp. 1033–1045, Oct. 2011, doi: 10.1016/j.jmbbm.2011.03.012.

[42] S. C. Scholes and A. Unsworth, “Wear studies on the likely performance of CFR-PEEK/CoCrMo for use as artificial joint bearing materials,” J Mater Sci: Mater Med, vol. 20, no. 1, p. 163, Aug. 2008, doi: 10.1007/s10856-008-3558-3.

[43] S. C. Scholes and A. Unsworth, “The wear performance of PEEK-OPTIMA based self-mating couples,” Wear, vol. 268, no. 3, pp. 380–387, Feb. 2010, doi: 10.1016/j.wear.2009.08.023.

[44] C. L. Brockett, G. John, S. Williams, Z. Jin, G. H. Isaac, and J. Fisher, “Wear of ceramic-on-carbon fiber-reinforced poly-ether ether ketone hip replacements,” Journal of Biomedical Materials Research Part B: Applied Biomaterials, vol. 100B, no. 6, pp. 1459–1465, 2012, doi: 10.1002/jbm.b.32664.

[45] T. M. Grupp et al., “Alternative bearing materials for intervertebral disc arthroplasty,” Biomaterials, vol. 31, no. 3, pp. 523–531, Jan. 2010, doi: 10.1016/j.biomaterials.2009.09.064.

[46] A. Milovanović, A. Sedmak, A. Grbović, T. Mijatović, and K. Čolić, “Design Aspects of Hip Implant Made of Ti-6Al-4V Extra Low Interstitials Alloy,” Procedia Structural Integrity, vol. 26, pp. 299–305, Jan. 2020, doi: 10.1016/j.prostr.2020.06.038.

[47] A. Milovanović, A. Sedmak, K. Čolić, T. U., and B. Đorđević, “Numerical analysis of stress distribution in total hip replacement implant,” Structural Integrity and Life, vol. 17, pp. 139–144, Oct. 2017.

[48] K. Colic, A. Sedmak, A. Grbovic, U. Tatic, S. Sedmak, and B. Djordjevic, “Finite Element Modeling of Hip Implant Static Loading,” Procedia Engineering, vol. 149, pp. 257–262, Jan. 2016, doi: 10.1016/j.proeng.2016.06.664.

[49] M. Babić, O. Verić, Ž. Božić, and A. Sušić, “Reverse engineering based integrity assessment of a total hip prosthesis,” Procedia Structural Integrity, vol. 13, pp. 438–443, Jan. 2018, doi: 10.1016/j.prostr.2018.12.073.

[50] A. Sedmak, K. Čolić, A. Grbović, I. Balać, and M. Burzić, “Numerical analysis of fatigue crack growth of hip implant,” Engineering Fracture Mechanics, vol. 216, p. 106492, Jul. 2019, doi: 10.1016/j.engfracmech.2019.106492.

[51] A. Sedmak and K. Čolić, “Fracture and Fatigue Behaviour of Implants Made of Ti Alloys,” Procedia Structural Integrity, vol. 23, pp. 45–50, Jan. 2019, doi: 10.1016/j.prostr.2020.01.061.

[52] M. Babić, O. Verić, Ž. Božić, and A. Sušić, "Fracture analysis of a total hip prosthesis based on reverse engineering," Engineering Fracture Mechanics, vol. 215, pp. 261–271, Jun. 2019, doi: 10.1016/j.engfracmech.2019.05.003.

[53] E. F. Morgan, G. U. Unnikrisnan, and A. I. Hussein, "Bone Mechanical Properties in Healthy and Diseased States," Annu Rev Biomed Eng, vol. 20, pp. 119–143, Jun. 2018, doi: 10.1146/annurev-bioeng-062117-121139.

[54] J. Sandler, P. Werner, M. S. P. Shaffer, V. Demchuk, V. Altstädt, and A. H. Windle, "Carbon-nanofibre-reinforced poly(ether ether ketone) composites," Composites Part A: Applied Science and Manufacturing, vol. 33, no. 8, pp. 1033–1039, Aug. 2002, doi: 10.1016/S1359-835X(02)00084-2.

[55] T. Pratap and K. Patra, "Tribological performances of symmetrically micro-textured Ti-6Al-4V alloy for hip joint," International Journal of Mechanical Sciences, vol. 182, p. 105736, Sep. 2020, doi: 10.1016/j.ijmecsci.2020.105736.

[56] "Titanium Alloys - Ti6Al4V Grade 5," AZoM.com, Jul. 30, 2002. https://www.azom.com/article.aspx?ArticleID=1547 (accessed Jul. 14, 2021).

[57] "ASM Material Data Sheet." http://asm.matweb.com/search/SpecificMaterial.asp?bassnum=MTP641 (accessed Jul. 14, 2021).

[58] S. A. Swanson, M. A. Freeman, and W. H. Day, "The fatigue properties of human cortical bone," Med Biol Eng, vol. 9, no. 1, pp. 23–32, Jan. 1971, doi: 10.1007/BF02474401.

[59] M. C. Sobieraj, J. E. Murphy, J. G. Brinkman, S. M. Kurtz, and C. M. Rimnac, "Notched fatigue behavior of PEEK," Biomaterials, vol. 31, no. 35, pp. 9156–9162, Dec. 2010, doi: 10.1016/j.biomaterials.2010.08.032.

[60] A. Z. Senalp, O. Kayabasi, and H. Kurtaran, "Static, dynamic and fatigue behavior of newly designed stem shapes for hip prosthesis using finite element analysis," Materials & Design, vol. 28, no. 5, pp. 1577–1583, Jan. 2007, doi: 10.1016/j.matdes.2006.02.015.

[61] G. Bergmann et al., "Hip contact forces and gait patterns from routine activities," J Biomech, vol. 34, no. 7, pp. 859–871, Jul. 2001, doi: 10.1016/s0021-9290(01)00040-9.

[62] G. Bergmann, F. Graichen, and A. Rohlmann, "Hip joint loading during walking and running, measured in two patients," J Biomech, vol. 26, no. 8, pp. 969–990, Aug. 1993, doi: 10.1016/0021-9290(93)90058-m.

[63] G. Bergmann, F. Graichen, and A. Rohlmann, "Hip joint contact forces during stumbling," Langenbecks Arch Surg, vol. 389, no. 1, pp. 53–59, Feb. 2004, doi: 10.1007/s00423-003-0434-y.

[64] 14:00-17:00, "ISO 7206-8:1995," ISO. https://www.iso.org/cms/render/live/en/sites/isoorg/contents/data/standard/02/10/21009.html (accessed Jul. 15, 2021).

[65] 14:00-17:00, "ISO 7206-4:2010," ISO. https://www.iso.org/cms/render/live/en/sites/isoorg/contents/data/standard/04/27/42769.html (accessed Jul. 15, 2021).

[66] J. R. Atkinson, D. Dowson, J. H. Isaac, and B. M. Wroblewski, "Laboratory wear tests and clinical observations of the penetration of femoral heads into acetabular cups in total replacement hip joints: III: The measurement of internal volume changes in explanted Charnley sockets after 2–16 years in vivo and the determination of wear factors," Wear, vol. 104, no. 3, pp. 225–244, Aug. 1985, doi: 10.1016/0043-1648(85)90050-X.

[67] J. Livermore, D. Ilstrup, and B. Morrey, "Effect of femoral head size on wear of the polyethylene acetabular component," J Bone Joint Surg Am, vol. 72, no. 4, pp. 518–528, Apr. 1990.

[68] J. M. Kabo, J. S. Gebhard, G. Loren, and H. C. Amstutz, "In vivo wear of polyethylene acetabular components," J Bone Joint Surg Br, vol. 75, no. 2, pp. 254–258, Mar. 1993, doi: 10.1302/0301-620X.75B2.8444946.

[69] R. M. Hall, A. Unsworth, P. Siney, and B. M. Wroblewski, "Wear in retrieved Charnley acetabular sockets," Proc Inst Mech Eng H, vol. 210, no. 3, pp. 197–207, 1996, doi: 10.1243/PIME_PROC_1996_210_413_02.

[70] J.-H. Chen and J. Shih-Shyn Wu, “Measurement of polyethylene wear - a new three-dimensional methodology,” Comput Methods Programs Biomed, vol. 68, no. 2, pp. 117–127, May 2002, doi: 10.1016/s0169-2607(01)00164-x.

[71] V. Saikko, P. Paavolainen, M. Kleimola, and P. Stätis, “A five-station hip joint simulator for wear rate studies,” Proc Inst Mech Eng H, vol. 206, no. 4, pp. 195–200, 1992, doi: 10.1243/PIME_PROC_1992_206_291_02.

[72] V. O. Saikko, “A three-axis hip joint simulator for wear and friction studies on total hip prostheses,” Proc Inst Mech Eng H, vol. 210, no. 3, pp. 175–185, 1996, doi: 10.1243/PIME_PROC_1996_210_410_02.

[73] A. Wang et al., “Orientation softening in the deformation and wear of ultra-high molecular weight polyethylene,” Wear, vol. 203–204, pp. 230–241, Mar. 1997, doi: 10.1016/S0043-1648(96)07362-0.

[74] A. Wang, C. Stark, and J. H. Dumbleton, “Mechanistic and morphological origins of ultra-high molecular weight polyethylene wear debris in total joint replacement prostheses,” Proc Inst Mech Eng H, vol. 210, no. 3, pp. 141–155, 1996, doi: 10.1243/PIME_PROC_1996_210_407_02.

[75] A. Wang, A. Essner, V. K. Polineni, C. Stark, and J. H. Dumbleton, “Lubrication and wear of ultra-high molecular weight polyethylene in total joint replacements,” Tribology International, vol. 31, no. 1, pp. 17–33, Jan. 1998, doi: 10.1016/S0301-679X(98)00005-X.

[76] Y. Q. Wang and J. Li, “Sliding wear behavior and mechanism of ultra-high molecular weight polyethylene,” Materials Science and Engineering: A, vol. 266, no. 1, pp. 155–160, Jun. 1999, doi: 10.1016/S0921-5093(99)00040-4.

[77] H. C. Meng and K. C. Ludema, “Wear models and predictive equations: their form and content,” Wear, vol. 181–183, pp. 443–457, Mar. 1995, doi: 10.1016/0043-1648(95)90158-2.

[78] H. Czichos, “Chapter 1 - Introduction to Friction and Wear,” in Composite Materials Series, vol. 1, K. Friedrich, Ed. Elsevier, 1986, pp. 1–23. doi: 10.1016/B978-0-444-42524-9.50005-3.

[79] J. M. Challen and P. L. B. Oxley, “An explanation of the different regimes of friction and wear using asperity deformation models,” Wear, vol. 53, no. 2, pp. 229–243, Apr. 1979, doi: 10.1016/0043-1648(79)90080-2.

[80] J. S.-S. Wu, J.-P.Hung, C.-S.Shu, and J.-H. Chen, “The computer simulation of wear behavior appearing in total hip prosthesis,” Computer Methods and Programs in Biomedicine, vol. 70, no. 1, pp. 81–91, Jan. 2003, doi: 10.1016/S0169-2607(01)00199-7.

[81] J.-P. Hung and J. S.-S.Wu, “A comparative study on wear behavior of hip prosthesis by finite element simulation,” Biomed. Eng. Appl. Basis Commun., vol. 14, no. 04, pp. 139–148, Aug. 2002, doi: 10.4015/S1016237202000218.

[82] Shailesh S. Pimpale , Manish S. Deshmukh, Rajesh T. Shelke and Dheeraj S.Deshmukh “Biomaterial Properties of Femur Implant on Acetabulum Erosion: A Review,” Journal of Biomimetics ,Biomaterials and Biomedical Engineering , Vol. 51, pp 39- 62, June 2021, doi:10.4028/www.scientific.net/JBBBE.51.39